Dalton Transactions

ROYAL SOCIETY OF CHEMISTRY

PAPER

View Article Online
View Journal | View Issue

Cite this: *Dalton Trans.*, 2025, **54**, 14896

New dithiooxamide derivatives as promising precursors for ALD/MLD applications

Parmish Kaur, [a] Mikko Nisula,[b] Christophe Detavernier [b] and Anjana Devi *[a,c,d,e]

Hybrid materials synthesized combining atomic layer deposition and molecular layer deposition (ALD/MLD) results in advantageous material properties owing to the functionalities contributed from the inorganic and organic constituents in the film. The number of MLD precursors that are volatile and compatible with ALD precursors are limited. This study explores the synthesis and characterization of new dithiooxamide (DTOA) derivatives with varied side chain lengths for their application in ALD/MLD processes for the fabrication of Cu-R DTOA thin films. Utilizing bis(dimethylamino-2-propoxy)-copper(II) (Cu(dmap)$_2$) as the metal precursor, the impact of side chain modifications on the thermal stability and volatility of DTOA derivatives was investigated. Employing complementary analytical tools namely NMR, FTIR and TGA/DSC, the study unveils the structural and thermal properties of synthesized derivatives. From the proof-of-concept ALD/MLD experiments performed, the *in situ* spectroscopic ellipsometry monitored deposition process demonstrates a controlled linear thickness increase with deposition cycles, affirming the suitability of the DTOA derivatives as MLD precursors. This study delineates the influence of alkyl side chain variation on precursor properties, offering insights into the tailored design of precursors for advanced material deposition.

Received 15th June 2025,
Accepted 9th September 2025

DOI: 10.1039/d5dt01405k

rsc.li/dalton

Introduction

The introduction of atomic layer deposition (ALD) processing of functional materials represents a significant breakthrough in thin film technology, offering an unparalleled approach to deposit films conformally with precisely engineered properties. These methodologies, distinguished by their capability to control film thickness and composition at an atomic level, have catalysed the development of semiconductors, catalytic systems, medical devices, displays and energy devices with enhanced performance.[1–3] The organic variation namely molecular layer deposition (MLD) extends the compositional scope to include organic films. When inorganic and organic precursors are combined to yield hybrid inorganic–organic thin films, the combined terminology ALD/MLD reflects the dual nature of the process, in which the inorganic half-cycles and the organic half-cycles opens new prospects in the realms of flexible electronics, gas separation technologies, and optoelectronics.[4–8] Its applications span a wide array of industries, from the enhancement of semiconductor devices to the innovation in catalysis and the advancement of surface coatings, thereby underscoring its role in modern material science.[9–13] A recent review article summarizes and highlights the importance of ALD/MLD processing of ALD and MLD layers for a range of functional applications.[14]

The properties of organic/hybrid metalorganic films depend on the choice of both inorganic and organic precursor molecules. These molecules serve as essential building blocks for creating the desired characteristics of materials, as they integrate into the film, distinguishing them from the metal precursors ligands used in ALD to make inorganic films. Achieving superior performance and precise control over material properties necessitates the chemical modification of organic molecules used in MLD. This modification not only enhances the molecule's physicochemical properties but also focuses on fine-tuning functional groups and molecular size to improve their thermal properties and reactivity. Such adjustments are crucial for ensuring the molecules are perfectly suited for MLD's precise and controlled deposition processes. Furthermore, this approach paves the way for customization of materials through detailed molecular engineering. The vast potential of MLD remains underutilized due to the limited

[a]*Inorganic Materials Chemistry, Ruhr University Bochum, Universitätsstr. 150, 44801 Bochum, Germany*
[b]*Department of Solid State Sciences, Ghent University, Ghent B-9000, Belgium*
[c]*Leibniz Institute for Solid State and Materials Research, IFW Dresden, Helmholtzstr. 20, 01069 Dresden, Germany. E-mail: a.devi@ifw-dresden.de*
[d]*Chair of Materials Chemistry, Faculty of Chemistry and Food Chemistry, TU Dresden, Bergstrasse 66, 01069 Dresden, Germany*
[e]*Fraunhofer Institute for Microelectronic Circuits and Systems (IMS), Finkenstr. 61, 47057 Duisburg, Germany*

attention given to the rational design of organic precursor molecules. Additionally, there is a small library of commercially available molecules with suitable physicochemical properties. Such constraints hinder the full exploration of MLD's potential to create materials with tailored characteristics.

Among hybrid materials, copper-based hybrid thin films are of particular interest due to copper's unique combination of redox activity, electrical conductivity, and catalytic behaviour.[15] When coordinated with suitable organic linkers, these films can offer tuneable physicochemical properties that are highly desirable for applications in electrocatalysis, thermoelectric materials, batteries, antimicrobial coatings, and nanoelectronics.[16–19]

The implementation of hybrid Cu–organic thin films using organic linkers such as hydroquinone (HQ), terephthalic acid (TPA), 4,4′-oxydianiline (ODA), *p*-phenylenediamine (PPDA), and 1,4-benzenedithiol (BDT) has demonstrated considerable promise; however, several intrinsic limitations of these precursors hinder their broader utility in MLD processes. Hagen *et al.*[20] demonstrated that these precursors exhibit a wide range of sublimation temperatures—approximately 100 °C for HQ, 160 °C for TPA, 140 °C for ODA, 70 °C for PPDA, and 35 °C for BDT—posing challenges in finding compatible metalorganic precursors. Another study showed use of TPA at 180 °C to get crystalline CuTPA films deposited at 190 °C.[21,22] In one notable case, the use of HQ in combination with bis(dimethylamino-2-propoxy)-copper(II) $Cu(dmap)_2$ led to the formation of metallic copper films when the deposition temperature exceeded 120 °C, indicating thermal decomposition and loss of MLD self-limiting behavior.[20] Similar formation of Cu film has been shown with other combinations of $Cu(dmap)_2$ with ODA at deposition temperature of 240 °C (ref. 20) and bis(2,2,6,6-tetramethyl-3,5-heptanedionate) copper(II) $Cu(thd)_2$ in combination with HQ at deposition temperature of 160–240 °C.[23,34]

Although there has been advances made in developing new ALD/MLD processes, there is more room for improvement especially the volatility, reactivity and thermal stability of organic precursors.

Addressing this gap, this research aims at investigating dithiooxamide (DTOA) derivatives as potential precursors for ALD/MLD applications. Dithiooxamide, alternatively recognized as rubeanic acid,[24] is a molecule exhibiting redox activity and a dibasic acidic nature, as depicted in Fig. S1. DTOA derivatives represent a promising class of organic precursors due to their rigid, planar backbone, multidentate coordination sites, and strong electron-donating thiocarbonyl groups, which enable stable complexation with transition metals such as copper. Its structural modularity allows for functional tuning through side-chain modifications, making them ideal candidates for use in ALD/MLD processes that demand both thermal robustness and tailored reactivity.

Recently, a 1D coordination polymer *N*,*N*′-dimethyl dithiooxamidato-copper thin films using ALD/MLD demonstrated high out-of-plane ordering and can transition from insulating to metallic conductivity upon reductive doping.[25] The orientation seems to play a vital role in determining the film properties. The influence of varied side chain lengths for the ALD/MLD is unknown.

With this study as a basis for further exploration of MLD precursors, we report on the synthesis and characterization of DTOA derivatives with the scope of making them compatible with ($Cu(dmap)_2$) to derive hybrid films of Cu *via* ALD/MLD. Our aim is to understand how variations in the side chain length of these derivatives affect their thermal stability and volatility—key factors for the effectiveness of ALD/MLD processes. The experimental part of this research outlines the synthesis of a series of DTOA derivatives, including methyl-DTOA (Me-DTOA) **1**, ethyl-DTOA (Et-DTOA) **2**, isopropyl-DTOA (iPr-DTOA) **3**, normal propyl-DTOA (nPr-DTOA) **4**, and normal butyl-DTOA (nBu-DTOA) **5**. Following synthesis, we conducted a detailed analysis of their structural and thermal properties using techniques such as nuclear magnetic resonance (NMR) spectroscopy, Fourier transform infrared spectroscopy (FTIR), thermogravimetric analysis and differential scanning calorimetry (TGA/DSC). Furthermore, proof-of-concept ALD/MLD depositions were performed using the DTOA derivatives (**2–5**) with ($Cu(dmap)_2$) as the Cu source, the details of which are described herein. We showcase the practical applicability of DTOA derivatives for ALD/MLD applications.

Experimental

The synthesis of all the DTOA compounds was done using under standard atmospheric conditions. NMR spectroscopy measurements were conducted using a Bruker AV III 300 spectrometer at a temperature of 298 K. Reference points for all signals were based on the residual proton signals found in deuterated solvent $CDCl_3$, and these were aligned with the standard values for tetramethylsilane (TMS). The obtained NMR spectra were analysed further using MestReNova software. For FTIR spectroscopy, a range of 400–4000 cm^{-1} was covered utilizing a PerkinElmer spectrum two device, equipped with an attenuated total reflectance (ATR) module, within an argon atmosphere glove box. TGA was executed using a Netzsch STA409 PC/PG instrument under normal pressure conditions, with a sample mass of approximately 10 mg in an alumina crucible of 6.15 mm diameter. The TGA process utilized a heating rate of 5 °C per minute and a nitrogen flow rate of 90 sccm supplied by Air Liquide (purity of 99.998%). Melting points were assessed using simultaneous DSC, with a unit measure of milliwatts per milligram (mW mg^{-1}). The vapor pressure calculations were made according to the procedure given by Price *et al.*[26] and stepped isothermal TGA.

The synthesis procedures for five DTOA derivatives, namely Me DTOA **1**, Et DTOA **2**, iPr DTOA **3**, nPr DTOA **4**, and nBu DTOA **5**, are described below. Each synthesis involved the reaction of dithiooxamide with different amines to yield the respective DTOA derivatives. The detailed synthesis is described as follows.

Synthesis of Me DTOA 1

0.3 g of dithiooxamide was dissolved in ethanol. To this, 2 mL of 33% methylamine solution (excess) in ethanol was added dropwise. The solution was stirred at 40 °C for one hour. Then the solution was cooled on an ice bath. 0.180 g of yellow precipitate obtained was filtered, washed with deionized (DI) water and dried. Yield = 49%; ^{1}H NMR δ (ppm) = 10.35(b) NH, 3.39(d) –CH_3; ^{13}C NMR δ (ppm) = 185.71 C═S, 34.31 –CH_3.

Synthesis of Et DTOA 2

0.8 g of dithiooxamide was added to 3 mL 70% solution of ethylamine in water. The solution turned from red to green. The solution was stirred at 40 °C for one hour and the color became reddish yellow. The yellow precipitate was obtained on cooling using ice bath and further filtered, washed with DI water and dried to obtain 0.6 g of Et DTOA. Yield = 51%; ^{1}H NMR δ (ppm) = 10.29(b) NH, 3.73(qd) –CH_2–, 1.37(t) –CH_3; ^{13}C NMR δ (ppm) = 184.44 C═S, 42.54 –CH_2–, 12.76 –CH_3.

Synthesis of iPr DTOA 3

1.14 mL of 99% isopropyl amine was added to 4 mL deionized water. 0.8 g of dithiooxamide was added to this solution resulting in orange solution. The solution was stirred at 40 °C for one hour. The yellow precipitate was obtained on cooling which was then washed with DI water and dried. 0.952 g of yellow precipitate of iPr DTOA was obtained after filtration. Yield = 70%; ^{1}H NMR δ (ppm) = 10.24(b) NH, 4.50(dhept) –CH, 1.35(d) –CH_3; ^{13}C NMR δ (ppm) = 183.28 C═S, 49.36 –CH, 20.88 –CH_3.

Synthesis of nPr DTOA 4

1 mL of 98% propylamine was cooled to 0 °C. 0.5 g of dithiooxamide was added step wise. The solution turned yellow and was stirred overnight and recrystallized in methanol at −30 °C. 0.2 g of orange-red product was obtained. Yield = 24%; ^{1}H NMR δ (ppm) = 10.38(b) NH, 3.66(td) –CH_2–, 1.79(m) –CH_2–, 1.03(t) –CH_3; ^{13}C NMR δ (ppm) = 184.62 C═S, 49.30 –CH_2–, 21.06 –CH_2–, 11.73 –CH_3.

Synthesis of nBu DTOA 5

2 mL of methanol was added to 1.68 mL of 99% butylamine solution. 1 g of dithiooxamide was added stepwise at room temperature. 2 mL of methanol was added further to the solution and stirred for one hour. The solution was cooled with an ice bath. The yellow precipitate was obtained, filtered and dried to obtain 0.507 g of nBu DTOA. Yield = 20%; ^{1}H NMR δ (ppm) = 10.35(b) NH, 3.69(td) –CH_2–, 1.75(m) –CH_2–, 1.45(m) –CH_2–, 0.98(t) –CH_3; ^{13}C NMR δ (ppm) = 184.52 C═S, 47.45 –CH_2–, 29.68 –CH_2–, 20.44 –CH_2–, 13.86 –CH_3.

Thin film deposition

The ALD/MLD experiments were performed in an in-house fabricated, pump-operated high-vacuum ALD reactor at University of Ghent, achieving a base pressure of 10^{-5} mbar. Si substrates were used for thin film deposition. Throughout the deposition procedure, the sample substrate temperature was precisely controlled at 80 °C, while the reactor chamber walls were maintained at 85 °C. As precursors, bis(dimethylamino-2-propoxy)-copper(II) ($Cu(dmap)_2$), (Strem Chemicals) and the synthesised DTOA derivatives were employed. The thin films thickness was measured by *in situ* spectroscopic ellipsometer and bonding was characterised by FTIR. The FTIR analyses on thin film samples were performed with a Bruker VERTEX 70 V spectrometer, featuring a DTGS detector, in transmission mode. The measurements were performed on the thin film samples on double-sided polished Si(100) wafers, and a spectrum from a blank Si wafer was subtracted to mitigate the background effects of the substrate, which was also adjusted for enhanced spectral comparison. The composition of thin films were measured with X-ray photoelectron spectroscopy (XPS). The measurements were performed on a Thermo Scientific Theta Probe tool with Al Kα radiation on a 0.3 mm diameter spot focused by a MXR1 monochromator. X-ray diffraction data was collected with a Bruker D8 diffractometer with Cu Kα radiation.

Results and discussion

The synthesis of dithiooxamide derivatives was accomplished through the reaction of dithiooxamide with various amines, resulting in the formation of the corresponding DTOA derivatives, Fig. 1. Although some of these compounds are reported for synthesis of organic molecules,[27–29] they were not explored as MLD precursors except for the case where Nisula *et al.* implemented *N*,*N*′-dimethyl dithiooxamidato-copper for the synthesis of one-dimensional (1D) coordination polymer.[25] Thus, it was important to synthesize the DTOA derivatives modifying the synthesis procedures and varying the side chains systemically with the perspective of using them as MLD precursors. Additionally, for the use of these compounds as precursors, it is relevant that the synthesis should be scalable which was also addressed in this study. The synthesis was carried out by the dissolution of dithiooxamide in an appropriate solvent followed by the addition of the amine. This mixture was subjected to stirring and subsequent cooling, leading to the formation of a precipitate. The purification process involved the isolation of the precipitate *via* filtration, which was then subjected to washing and drying procedures to obtain the purified derivative. Fig. 2 illustrates the appearance of these compounds stored in vials, maintained at standard ambient temperature and pressure conditions. Notably, these compounds emanate a pungent odor attributable to the sulfur content within their molecular structure.

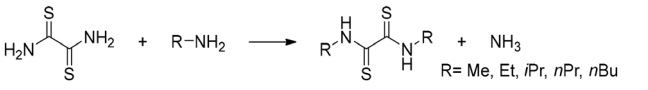

Fig. 1 Synthesis scheme for the preparation of dithiooxamide derivatives.

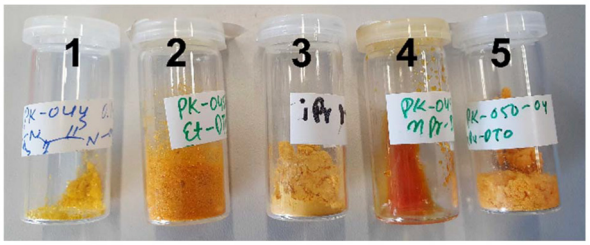

Fig. 2 Vials showing the synthesized DTOA derivatives **1–5**.

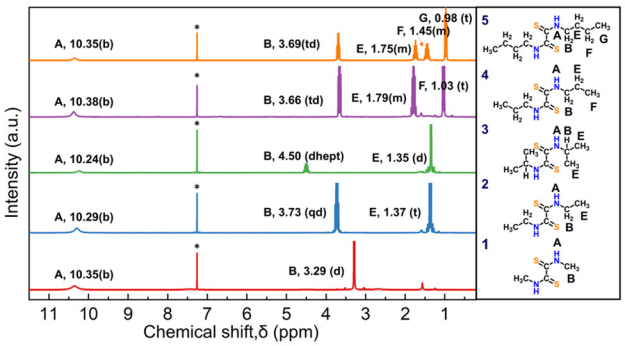

Fig. 3 ^{1}H NMR of DTOA derivatives (**1–5**) in $CDCl_3$. * = 7.26 ppm, 300 MHz.

Fig. 3 presents the ^{1}H NMR spectra of derivatives of dithiooxamide **1–5**, showcasing a diverse array of chemical shifts and multiplicity patterns that indicate a variety of proton environments within the molecular structures. The multiplicity of each signal is indicative of the complex splitting patterns resulting from spin–spin coupling between non-equivalent protons. For instance, the signals denoted by A, occurring between 10.24 ppm and 10.38 ppm, are characteristic of protons in a highly deshielded environment, which is associated with hydrogen atoms bonded to nitrogen in a thioamide functional group. These signals exhibit singlet patterns, suggesting the absence of neighboring protons that would induce splitting. The series of peaks labeled B, ranging from 3.29 ppm (doublet) to 4.50 ppm (doublet of heptets), reflect protons in varying environments and are influenced by the alkyl chains or amide hydrogen. The complexity of these patterns (doublets, triplets, and quartets) corresponds to the number of adjacent protons.

Signals E and F, with chemical shifts from 1.03 ppm to 1.79 ppm, represent protons in less deshielded environments, typical for protons attached to carbons that are farther away from the electronegative sulfur atoms or involved in aliphatic chains. The peak at G, near 0.98 ppm, is a triplet indicating a methyl group ($-CH_3$) with two neighboring protons, at the end of butyl alkyl chain.

Fig. 4 is a ^{13}C NMR spectra of derivatives of dithiooxamide **1–5**, displaying a range of chemical shifts that offer insight into the carbon environments within the molecular frameworks. The signals are classified as A, B, E, F, and G, each correlating to distinct carbon environments in the compounds' structures. The

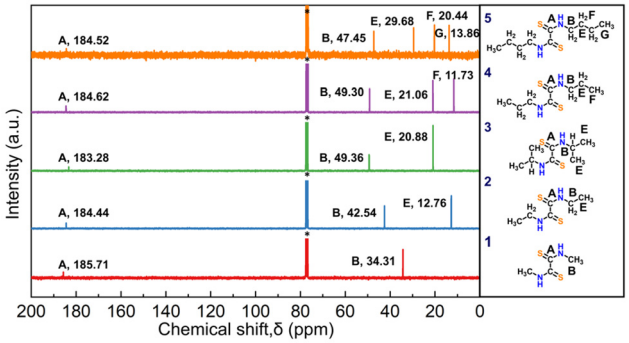

Fig. 4 ^{13}C NMR of DTOA derivatives (**1–5**) in $CDCl_3$. * = 77.16 ppm, 300 MHz.

peaks denoted by A, with chemical shifts from 183.28 ppm to 185.71 ppm, are in the region characteristic of carbon atoms with a significant degree of deshielding and correspond to thioamide linkages. The high chemical shift values suggest these carbons are strongly influenced by the presence of adjacent electronegative sulfur atoms. Peaks labeled B, ranging from 34.31 ppm to 49.36 ppm, correspond to carbon atoms adjacent to nitrogen atoms, illustrating a less deshielded environment compared to the thioamide but influenced by electronegative atoms. The signals assigned to E, at 20.88 ppm and 21.06 ppm, and F, at 17.73 ppm, are indicative of aliphatic carbon environments, which are expected to appear at a lower chemical shift range. These may represent carbon atoms further away from the electronegative sulfur and nitrogen atoms and are part of alkyl side chains. Lastly, the peak marked G at 13.86 ppm is typical for methyl carbons, suggesting a terminal position in an alkyl chain and has almost no influence on the electronegativity of thioamide group.

Based on these findings, the ^{1}H and ^{13}C NMR spectra offer a comprehensive profile of the dithiooxamide derivatives, underlining the successful introduction of different amines to modify the parent DTOA structure and achieve a range of derivatives **1–5**. The combined data from these spectra confirms the chemical structures of synthesized compounds.

Further, the thermal characteristics which is an important figure of merit for ALD/MLD processes of the DTOA and its derivatives **1–5** were investigated. TGA was carried out as depicted in Fig. 5. The amount of weight change as the compound is heated, thermal stability, and the melting point are measured with TGA/DSC. From the plot, it's apparent that all compounds undergo significant weight loss upon heating, which is attributed to the volatility of these compounds. This is an important finding as the compounds sublime at lower temperatures even under atmospheric conditions (ambient pressure).

Table 1 shows the melting points of dithiooxamide (DTOA) and its derivatives as determined by DSC measurements. A significant decrease in melting point upon derivatization from the parent DTOA compound is observed. The parent compound DTOA has a relatively high melting point of 238–240 °C, indicating strong intermolecular forces due to hydrogen bonding. The

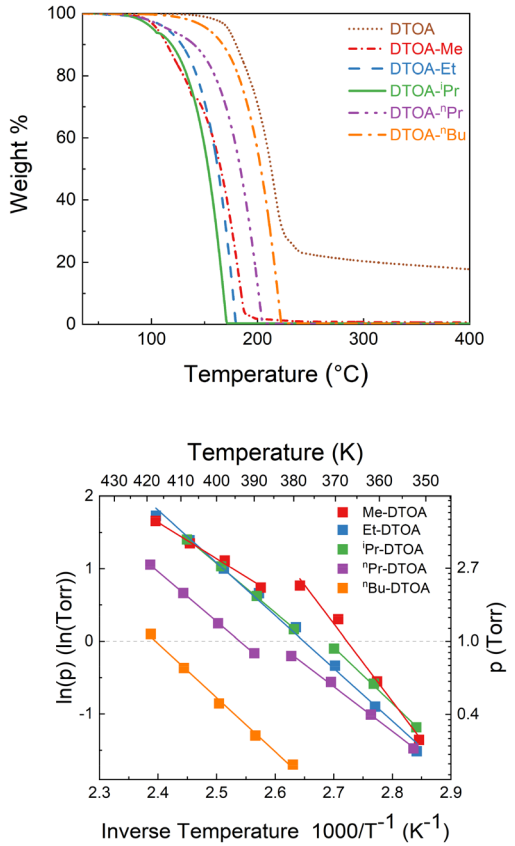

Fig. 5 TGA and vapor pressure plots of DTOA and compounds **1–5**.

introduction of a methyl group in **1** result in a much lower melting point of 135 °C. This is due to the methyl group introducing steric hindrance, decreasing intermolecular hydrogen bonding, which lowers the melting point. The ethyl derivative **2** has an even lower melting point of 56 °C. As the alkyl chain length is increasing, the molecular weight is increasing, but the melting point is decreasing. This suggests that while van der Waals forces increase with longer chains, the effect of disrupting the crystal lattice structure is more significant, leading to lowering of the melting point. Compound **3** exhibits a melting point of 102 °C. The isopropyl group is larger than the methyl and ethyl groups, which increases van der Waals interactions but also contributes to lowering of the hydrogen bonding in comparison to parent DTOA. Compound **4** is a liquid at room temperature, implying a melting point below 25 °C (room temperature). The normal propyl group extends the carbon chain further, which in the case of **4**, seems to lead to a molecular structure that does not solidify at room temperature, indicating very weak intermolecular forces in the solid state. The normal butyl derivative **5** has a melting point of 38 °C. This indicates that the longer butyl chain significantly reduces the intermolecular hydrogen bonding. The trend observed here—decreasing melting points with increasing alkyl chain length—suggests that the alkyl substituents decrease the hydrogen bonding that stabilize the crystal lattice of the parent DTOA compound. While longer alkyl chains can increase van der Waals forces, the decrease of intermolecular hydrogen bonding and increased molecular volume seem to play a dominant role in reducing the melting points of these derivatives.

The relative thermal stability and volatility was analysed by TGA for dithiooxamide (DTOA) and its alkyl-substituted derivatives **1–5**. DTOA itself demonstrates the highest onset of volatilization at 149 °C, which is due to strong intermolecular hydrogen bonding. Conversely, the compound **1** and **2** derivatives have substantially lower onset temperatures, at 88 °C and 82 °C respectively, indicating that even short-chain alkyl substitutions can substantially increase the volatility due to decrease in intermolecular hydrogen bonding. Compounds **3** and **4** having same molecular weight show similar behaviour, with onset temperatures of 81 °C and 85 °C, respectively, illustrating a continued trend of increased volatility with alkyl substitution. However, compound **5** exhibits a higher onset temperature of 121 °C, due to increased molecular weight and increased van der Waals forces. The absence of residual weight in DTOA derivatives **1–5** following thermal analysis suggests a complete volatilization through evaporation or sublimation without evidence of thermal decomposition. This contrasts with the parent DTOA, which retains 13% residual weight, indicating thermal decomposition. The complete volatilization of DTOA derivatives **1–5** is particularly advantageous in MLD processes where residue-free volatilization is desirable to ensure the purity and quality of the deposited layers.

Vapor pressure is a crucial parameter for evaluating the thermal characteristics of precursors. Fig. 5 (bottom) illustrates an Arrhenius-type plot, derived from the Clausius–Clapeyron relation, which is used to analyse the vapor pressures of compounds with change in temperature. This graph facilitates the extrapolation of the vapor pressure at different temperatures, including the temperature at which the vapor pressure reaches 1 Torr. This was determined as described by Price *et al.*[26] and the

Table 1 Thermal properties of the compounds **1–5** in comparison to DTOA

Compound	Melting point (°C)	Onset of volatilization (°C)	Residual weight (%)	Temperature in K at 1 Torr VP	Temperature °C at 1 Torr VP
DTOA	238–240	149	13	—	—
DTOA-Me (**1**)	135	88	0	367	94
DTOA-Et (**2**)	56	82	0	377	104
DTOA-iPr (**3**)	102	81	0	372	99
DTOA-nPr (**4**)	Liquid	85	0	394	121
DTOA-nBu (**5**)	38	121	0	414	141

values are given in Table 1. The various DTOA derivatives **1–5**, show that different substituents affect the vapor pressure of each compound. The compounds **1–3**, shows higher volatility than compounds **4** and **5** as the larger the alkyl group, the lower the vapor pressure at a given temperature due to the increased molecular weight and van der Waals forces. The change of the slopes of the vapor pressure can be attributed to changes in the thermal event such as melting, phase change or boiling.

In summary, the thermal analysis provides valuable insights into the thermal behaviour of DTOA and its derivatives **1–5**, demonstrating the influence of chemical modification on the compounds' volatility, thermal stability and decomposition characteristics. The modification of DTOA precursors through the introduction of different alkyl groups successfully enhanced their thermal properties, making them very appealing for ALD/MLD processes, which prompted us to

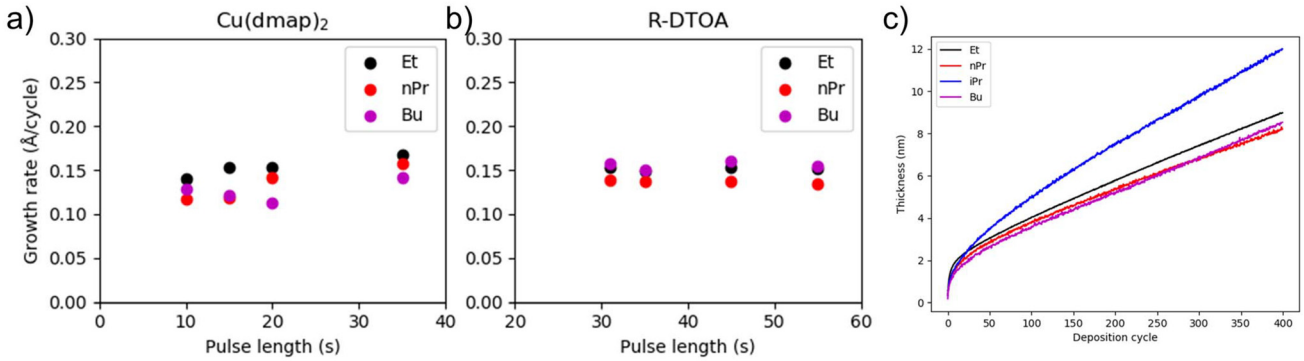

Fig. 6 Growth per cycle of the Cu-R DTOA films against pulse length, for (a) $Cu(dmap)_2$ and (b) R DTOA; (c) thickness *vs.* deposition cycles for Cu-R DTOA tracked through *in situ* ellipsometry. For $Cu(dmap)_2$ saturation studies, the R-DTOA pulse length was kept fixed at 35 s, and for R-DTOA saturation, the $Cu(dmap)_2$ pulse length was fixed to 20 s.

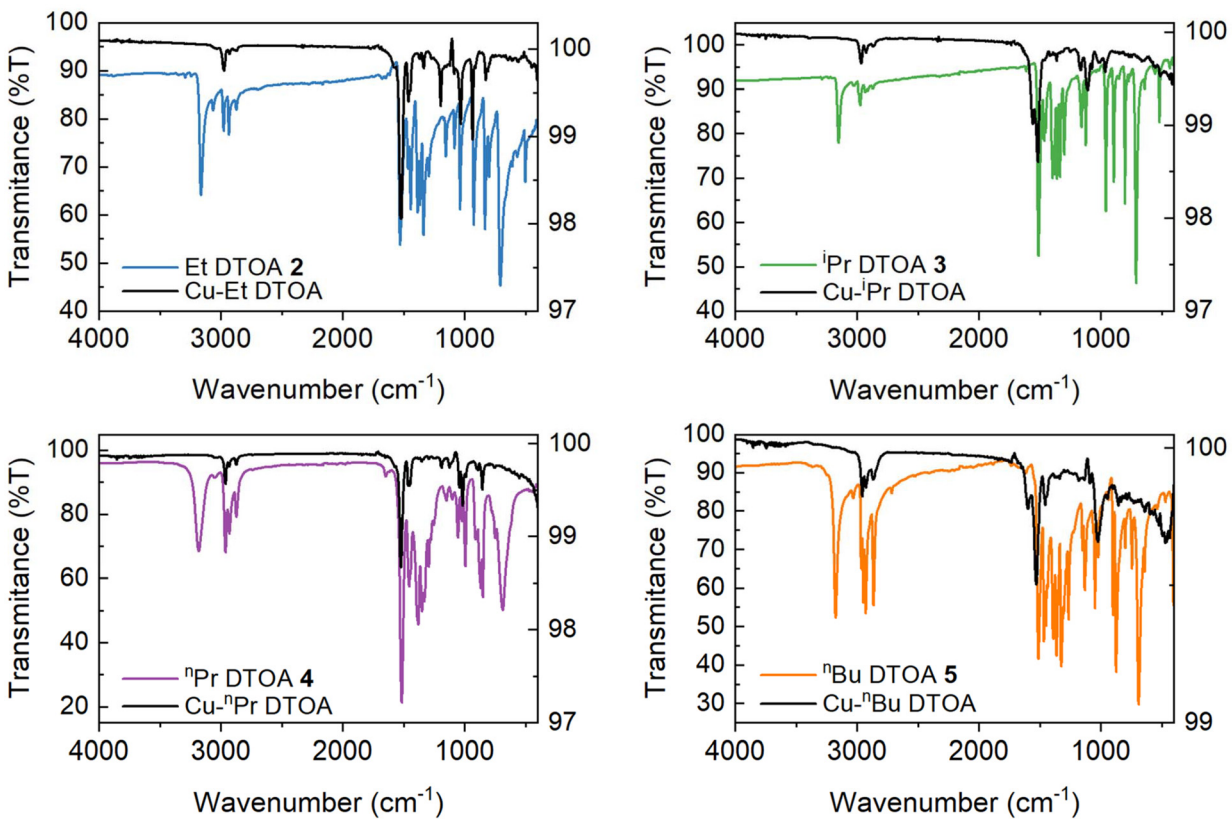

Fig. 7 FTIR of DTOA derivative **2–5** and their respective hybrid films. The horizontal axis represents wavenumber (cm^{-1}) and the vertical axis represents transmittance (%). The left vertical scale corresponds to the organic precursors, while the right vertical scale corresponds to the hybrid thin films.

employ them in Cu-based hybrid thin films *via* ALD/MLD as discussed in the following section.

ALD/MLD of Cu-R DTOA

To validate the suitability of DTOA derivatives **2–5** in ALD/MLD applications, proof-of-concept experiments were conducted using bis(dimethylamino-2-propoxy)-copper(II) ($Cu(dmap)_2$) as the metal precursor, at deposition temperatures as low as 80 °C on Si substrates as illustrated in Fig. 6. The deposition process underwent real-time monitoring *via* spectroscopic ellipsometry, which revealed a consistent and well-regulated increase in film thickness proportional to the number of deposition cycles, following an initial phase of accelerated growth. Notably, the growth per cycle (GPC) exhibited a saturation trend when the precursor pulse duration exceeded 10 seconds for $Cu(dmap)_2$ and 30 seconds for the dithiooxamide derivatives **2**, **4** and **5** (R DTOA) precursors, indicating a threshold beyond which no further increase in film thickness occurs with extended precursor exposure.

Additionally, FTIR spectroscopy was utilized to analyze Cu-R DTOA films in comparison to R DTOA derivatives, as illustrated in Fig. 7. FTIR spectra identify molecular functional groups through the absorption of infrared radiation, leading to molecular vibrations. These spectra are displayed as percent transmittance against wavenumber (measured in cm^{-1}). In the spectra, the black lines denote the infrared spectra of Cu-R DTOA thin films, while the colored lines represent the R DTOA compounds.[30–32]

The absence of strong N–H bands in the range of 3151–3181 cm^{-1} and 1363–1386 cm^{-1} suggests the substitution of the N–H bond with metal coordination in the Cu-R DTOA thin films. Furthermore, the retention of certain bands, which are fundamental to the compound's structure, indicates the preservation of the thioamide backbone in the thin film, a conclusion supported by Desseyn *et al.*[33] The presence of C–S and C–N bands, observable in both Cu-R DTOA thin films and R DTOA spectra around 1000 cm^{-1} and 1500 cm^{-1} respectively, further corroborates the structural integrity of these compounds within the films. Compositional analysis by XPS, Fig. S2 reveals that the derivatives **2** and **4** yield films are close to the expected chemical composition with only a small amount of oxygen impurity. On the other hand, the oxygen content of the films deposited from **3** and **5** is significant. This would suggest that these samples are more readily oxidized when exposed to an ambient atmosphere.

XRD measurements of the as-deposited films reveal a single prominent diffraction reflections for Et-DTOA and nPr-DTOA – based films, whereas iPr-DTOA and iBu-DTOA – based films appear to be amorphous (Fig. 8). For Et-DTOA and nPr-DTOA, the reflection position corresponds to *d*-spacing of 9.2 Å and 12.1 Å, respectively. In a previous study on Cu-MeDTOA, a structural motif with formation of polymeric 1D Cu-MeDTOA chains.[25] These would further stack into a sheet-like secondary structure with the alkyl groups separating adjacent sheets. The increasing *d*-spacing value with the increasing chain length of the alkyl substituent found in this study would thus be consistent with increasing intermolecular spacing of the adjacent polymeric chains.

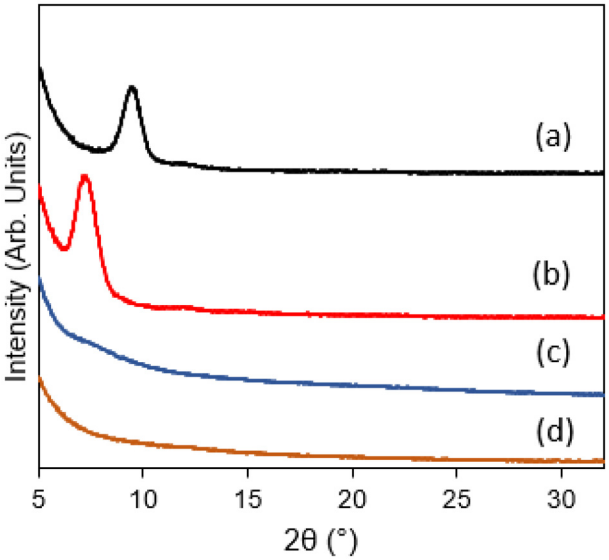

Fig. 8 X-ray diffractograms of (a) Et-DTOA, (b) nPr-DTOA, (c) iPr-DTOA, and (d) nBu-DTOA based Cu-R DTOA thin films deposited on Si substrates.

Conclusions

This study demonstrates for the first time the successful exploration of DTOA derivatives as suitable precursors for ALD/MLD. The potential of DTOA derivatives as versatile precursors for ALD/MLD processes, emphasizing the significance of side chain length variation on the thermal behaviour and successful low temperature ALD/MLD is presented. The DTOA derivatives exhibit superior thermal properties in terms of compounds either as liquids or low-melting-point solids and enhanced volatility compared to standard MLD precursors, rendering them highly conducive to their application in synthesizing Cu-R DTOA thin films. The meticulous analysis of structural, thermal, and deposition characteristics reveals the crucial role of molecular engineering in optimizing precursor performance for material deposition. *In situ* ellipsometry and FTIR spectroscopy during ALD/MLD processing further validate controlled film growth while maintaining structural integrity within the films. This study not only broadens the repertoire of precursors available for ALD/MLD but also sheds light on the strategic modification of organic molecules for the advancement of thin film technology.

The ability to modify the thermal properties of DTOA through molecular engineering opens new avenues for material design and the fabrication of thin films with customized properties. Moreover, by the use of DTOA derivatives, a successful method to fabricate the hybrid materials *via* ALD/MLD without the solvent inclusion, which are normally captured in the lattice with other preparation methods like solvo-

thermal synthesis, is a significant advantage. Further work needs to be carried out on the thorough characterization of deposited films to further understand their composition, structure, morphology, and exploring the functionalities for potential applications of the hybrid materials.

Conflicts of interest

There are no conflicts to declare.

Data availability

The data supporting this article have been included as part of the SI. Supplementary information is available. See DOI: **https://doi.org/10.1039/d5dt01405k**.

Acknowledgements

This project has received funding from the European Union's Horizon 2020 Research and Innovation programme under the Marie Skłodowska-Curie grant agreement (no. 765378 and 841995). P. K. thanks the EU-ITN-HYCOAT project for the early-stage researcher (ESR) fellowship. AD thanks RUB, the Leibniz Association (ASPIRE-2D project-P155/2023), and Fraunhofer Society (Attract Project-Grant No. Attract 40-00643) for supporting this work.

References

1 R. W. Johnson, A. Hultqvist and S. F. Bent, *Mater. Today*, 2014, **17**, 236–246.
2 J. A. Oke and T. C. Jen, *J. Mater. Res. Technol.*, 2022, **21**, 2481–2514.
3 P. O. Oviroh, R. Akbarzadeh, D. Pan, R. A. M. Coetzee and T. C. Jen, *Sci. Technol. Adv. Mater.*, 2019, **20**, 465–496.
4 T. S. Tripathi and M. Karppinen, *Adv. Mater. Interfaces*, 2017, **4**, 1–16.
5 P. Sundberg and M. Karppinen, *Beilstein J. Nanotechnol.*, 2014, **5**, 1104–1136.
6 J. Multia and M. Karppinen, *Adv. Mater. Interfaces*, 2022, **9**, 2200210.
7 A. Ghazy, D. Zanders, A. Devi and M. Karppinen, *Adv. Mater. Interfaces*, 2024, **2400274**, 1–30.
8 D. J. Hagen, M. E. Pemble and M. Karppinen, *Appl. Phys. Rev.*, 2019, **6**, 041309.
9 K. Ashurbekova, K. Ashurbekova, G. Botta, O. Yurkevich, M. Knez and M. Knez, *Nanotechnology*, 2020, **31**, 342001.
10 H. Van Bui, F. Grillo and J. R. Van Ommen, *Chem. Commun.*, 2017, **53**, 45–71.
11 X. Meng, *J. Mater. Chem. A*, 2017, **5**, 18326–18378.
12 H. Zhou and S. F. Bent, *J. Vac. Sci. Technol., A*, 2013, **31**, 040801.
13 B. Zhang, Z. Wang, J. Wang and X. Chen, *Micromachines*, 2024, **15**, 1–30.
14 M. Heikkinen, R. Ghiyasi and M. Karppinen, *Adv. Mater. Interfaces*, 2025, **12**, 2400262.
15 Z. Li, S. Chang, S. Khuje and S. Ren, *ACS Nano*, 2021, **15**, 6211–6232.
16 A. S. Sabir, E. Pervaiz, R. Khosa and U. Sohail, *RSC Adv.*, 2023, **13**, 4963–4993.
17 P. Qiu, X. Shi and L. Chen, *Energy Storage Mater.*, 2016, **3**, 85–97.
18 Y. Chen, Y. Zhang, Q. Huang, X. Lin, A. Zeb, Y. Wu, Z. Xu and X. Xu, *ACS Appl. Energy Mater.*, 2022, **5**, 7842–7873.
19 D. Mitra, E.-T. Kang and K. G. Neoh, *ACS Appl. Mater. Interfaces*, 2020, **12**, 21159–21182.
20 D. J. Hagen, L. Mai, A. Devi, J. Sainio and M. Karppinen, *Dalton Trans.*, 2018, **47**, 15791–15800.
21 B. Gikonyo, F. Liu, S. De, C. Journet, C. Marichy and A. Fateeva, *Dalton Trans.*, 2023, **52**, 211–217.
22 E. Ahvenniemi and M. Karppinen, *Chem. Commun.*, 2016, **52**, 1139–1142.
23 T. S. Tripathi and M. Karppinen, *Chem. Mater.*, 2017, **29**, 1230–1235.
24 C. D. Hodgman and S. C. Lind, *J. Phys. Colloid Chem.*, 1949, **53**, 1139–1139.
25 M. Nisula, A. J. Karttunen, E. Solano, G. C. Tewari, M. Karppinen, M. Minjauw, H. S. Jena, P. Van Der Voort, D. Poelman and C. Detavernier, *ACS Appl. Mater. Interfaces*, 2021, **13**, 10249–10256.
26 D. M. Price, *Thermochim. Acta*, 2001, **367–368**, 253–262.
27 R. N. Hurd, G. De La Mater, G. C. McElheny, R. J. Turner and V. H. Wallingford, *J. Org. Chem.*, 1961, **26**, 3980–3987.
28 H. Hoppe and K. Hartke, *Arch. Pharm.*, 1975, **308**, 526–541.
29 J. Voss, *Liebigs Ann. Chem.*, 1974, 1220–1230.
30 M. A. Deveci and G. Irez, *Synth. React. Inorg. Met.-Org. Chem.*, 1994, **24**, 1763–1771.
31 H. O. Desseyn, N. Blaton, B. Slootmaekers and S. P. Perlepes, *Spectrochim. Acta, Part A*, 2003, **59**, 1359–1372.
32 B. Slootmaekers, S. P. Perlepes and H. O. Desseyn, *Spectrochim. Acta, Part A*, 1996, **52**, 375–377.
33 H. O. Desseyn, W. A. Jacob and M. A. Herman, *Spectrochim. Acta, Part A*, 1969, **25**, 1685–1692.
34 T. S. Tripathi, M. Wilken, C. Hoppe, T. de los Arcos, G. Grundmeier, A. Devi and M. Karppinen, *Adv. Eng. Mater.*, 2021, **23**, 2100446.